Holzforschung, Vol. 63, pp. 589–596, 2009 • Copyright © by Walter de Gruyter • Berlin • New York. DOI 10.1515/HF.2009.100

Non-destructive determination and quantification of diffusion processes in wood by means of neutron imaging

David Mannes[1,2,*], Walter Sonderegger[1], Stefan Hering[1], Eberhard Lehmann[2] and Peter Niemz[1]

[1] Department of Civil, Environmental and Geomatic Engineering, Institute for Building Materials, Zurich, Switzerland

[2] Spallation Neutron Source (ASQ), Paul Scherrer Institute (PSI), Villigen, Switzerland

*Corresponding author.
Department of Civil, Environmental and Geomatic Engineering, Institute for Building Materials, ETH Zurich, 8093 Zurich, Switzerland
Phone: +41-44-632-3228
Fax: +41-44-632-1174
E-mail: dmannes@ethz.ch

Abstract

Diffusion processes in samples of European beech (*Fagus sylvatica* L.) and Norway spruce (*Picea abies* [L.] Karst.) were determined and quantified by means of neutron imaging (NI). The experiments were carried out at the neutron imaging facility NEUTRA at the Paul Scherrer Institute in Villigen (Switzerland) using a thermal neutron spectrum. NI is a non-destructive and non-invasive testing method with a very high sensitivity for hydrogen and thus water. Within the scope of this study, diffusion processes in the longitudinal direction were ascertained for solid wood samples exposed to a differentiating climate (dry side/wet side). With NI it was possible to determine the local distribution and consequently the total amount of water absorbed by the samples. The calculated values scarcely differ from those ascertained by weighing ($\leq$3%). The method yields profiles of the water content over the whole sample, thus allowing the local and temporal resolution of diffusion processes within the sample in the main transport direction (longitudinal). On the basis of these profiles, it was possible to calculate the diffusion coefficients along the fibre direction according to Fick's second law.

Keywords: diffusion; diffusion coefficient; moisture content; neutron imaging; non-destructive testing; wood.

Introduction

Since all wood properties (e.g., mechanical properties, heat conductivity, etc.) depend to a certain degree on the moisture content (MC), the interaction between wood and water is crucial for the utilisation of wood and wood based composites. Wood-water relations thus have long since been the focus of many investigations (e.g., Skaar 1988; Wadsö 1994; Siau 1995; Koc et al. 2003; Olek et al. 2005; Frandsen et al. 2007). Conventional destructive experimental methods applied in this context do not yield spatial information on water distribution within an object (e.g., standard diffusion experiment with regular weighing) or are of limited precision and their evidence is restricted to layers close to the surface (e.g., measurements based on electrical conductivity).

Experimental assessment of moisture distribution and transport processes is particularly difficult by destructive methods (Plagge et al. 2006). Non-destructive testing methods are more suitable. Most frequently, X-ray transmission measurements are applied. This approach includes evaluating computed tomographies (CTs) (Wiberg and Morén 1999; Alkan et al. 2007; Scheepers et al. 2007) and X-ray densitometry (Baettig et al. 2006; Cai 2008; Watanabe et al. 2008). Nuclear magnetic resonance (NMR) is also a promising method in this context (Merela et al. 2009).

Neutron imaging (NI) is a relatively new method, which has the same working principle as the X-ray methods. NI seems to be particularly suitable for moisture-related investigations as its sensitivity for hydrogen is considerably higher than that of X-ray photons (Lehmann et al. 2001a). Niemz et al. (2002) demonstrated the general suitability of NI for detecting moisture in wooden corner joints.

The goal of the present work is to show the possibilities of NI as a tool for time-dependent investigations on wood-water relations. The transport of moisture by diffusion in a differential climate was quantified and localised by means of NI on samples of European beech (*Fagus sylvatica* L.) and Norway spruce (*Picea abies* [L.] Karst.) over several hours. Diffusion coefficients in the longitudinal direction were calculated based on the results obtained.

Material and methods

The wood specimens were exposed to a differentiating climate (wet condition on one side, dry condition on the other) and time-dependent experiments about the moisture movement were performed. NI yields not only information on the quantity of the absorbed water but also on its spatial distribution.

Material

Two cuboid samples from European beech (*Fagus sylvatica* L.) and Norway spruce (*Picea abies* [L.] Karst.) with sizes of $5.0 \times 6.4 \times 2.0$ cm^3 and densities of 0.65 g cm^{-3} and 0.38 g cm^{-3}, respectively, were tested. The oven-dry samples (dried at 103°C until weight constancy) were isolated with aluminium tape on four sides, leaving only the opposite sides unsealed (the radial-tangential planes), so that only the longitudinal diffusion direction was permitted. The samples were then fixed on a box of acrylic glass filled with silica gel as the desiccating agent. One unsealed surface of the samples was connected with the inner dry climate of the box via rectangular openings in the lid, which were slightly

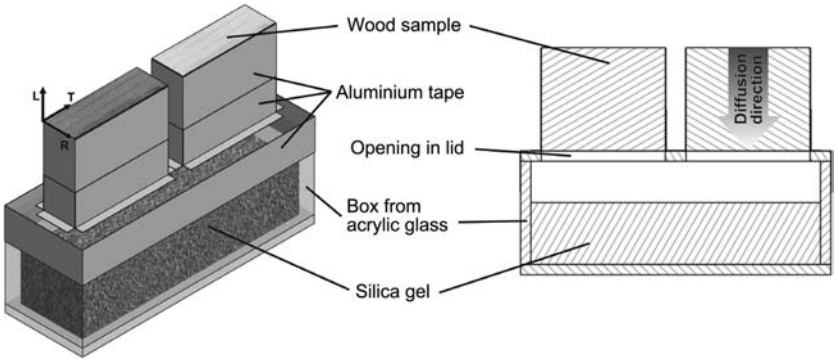

Figure 1 The samples were isolated on four sides with overlapping aluminium tape and then fixed above openings on a box containing silica gel as dehydrating agent; moisture uptake occurred exclusively over the cross-section, diffusion was only possible in longitudinal direction; L, R, T = longitudinal, radial, tangential direction.

smaller than the size of the adjacent specimens. Gaps between box and specimen, as well as between box and lid, were sealed with aluminium tape (Figure 1).

Methods

Experimental setup The experiments were performed at the NI facility NEUTRA at the Paul Scherrer Institute (PSI) in Villigen, Switzerland. This imaging beam-line is fed by the Spallation Neutron Source SINQ and operates with neutrons in a thermal spectrum (Lehmann et al. 2001b).

The climatic conditions around the samples had to be regulated during the experiments. For this purpose, a climatic chamber was built, in which the specimens were placed during the experiment (Figure 2). The chamber consisted of acrylic glass and had two neutron-transparent windows of plain glass. The climate was regulated with two basins filled with demineralised water or saturated salt solutions (depending on the desired humidity), two Peltier elements with cooling fins and two ventilators. Two sensors recorded the temperature and relative humidity (RH). The climate reached during the actual experiment was 27°C at 86% RH.

The chamber was positioned in front of the neutron detector, which consisted of a scintillator-CCD-camera system with a field of view of 130 mm. The scintillator (zinc sulphide doped with lithium-6 as neutron absorbing agent) converts the neutron signal into visible light, which is led via a mirror onto a cooled 16-bit CCD camera (resolution: 1024×1024 pixels), which registers the signal. The exposure time was 240 s/image. The conditioning of the chamber was initiated while the samples were being prepared (i.e., isolation of the sides and fixing on the box containing the silica gel) so that an almost stable climate in the chamber was attained, when the samples were inserted. However, to position the samples within the chamber it had to be opened, thus the air conditioning was interrupted for that period. After this, it took approximately 30 to 40 min for climate stabilisation.

To obtain a reference image of the dry samples, the experiment was started right after the samples were placed into the climatic chamber. From then on, images were taken every 15 min over the period of 39 h. The conditions in the climatic chamber were only stable for the first 8 h. Hence, only this part of the experiment was taken into account to determine the water absorption.

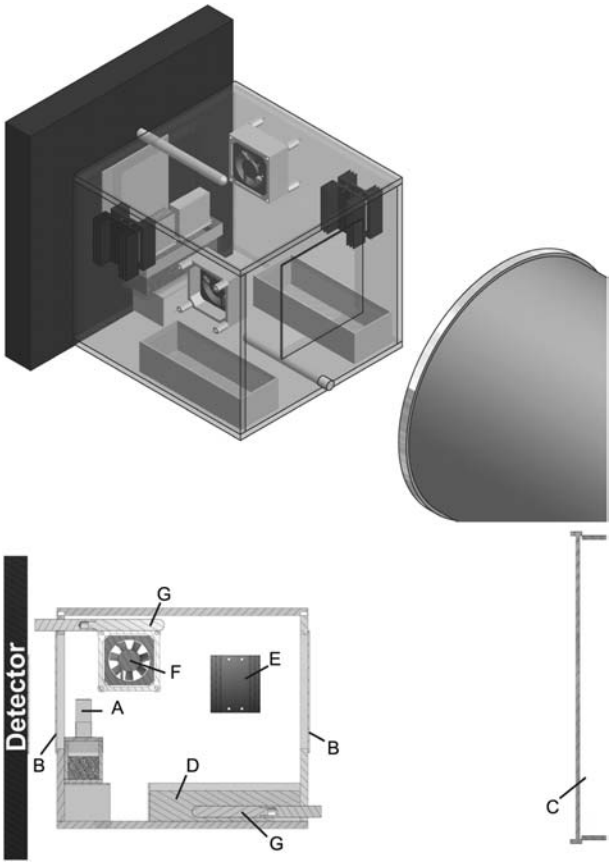

Figure 2 General view (top) and sectional view (bottom) of the experimental setup: the samples (A; compare to Figure 1) are placed in the climatic chamber with neutron transparent windows (B). The chamber is positioned between the evacuated flight tube (C) and the neutron detector; relative humidity and temperature are regulated by basins filled with water (D) and Peltier elements with cooling ribs (E). Ventilators (F) are perturbed the air, while the climatic conditions are registered with thermo-hygrometric sensors (G).

General principle NI is based on the intensity measurement of a neutron beam transmitted through an object, thus integrating the objects properties in the direction of the beam. The intensity of the transmitted beam I can be described in a first order approach with the linear attenuation law:

$$I = I_0 \, e^{-\Sigma \cdot z}, \tag{1}$$

where I_0 is the intensity of the incident neutron beam, Σ is the attenuation coefficient and z is the thickness of the object in the beam direction (Figure 3). Σ is the main parameter describing the degree to which a material interacts and attenuates the neu-

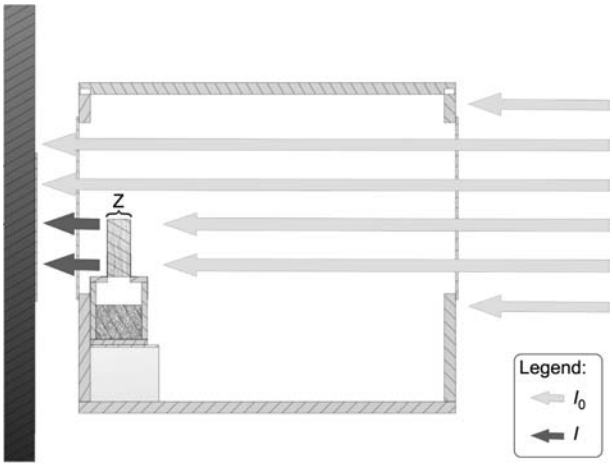

Figure 3 Neutron radiation with the intensity I_0 is sent onto the sample with the thickness z, which was placed in a climatic chamber. The transmitted beam with the intensity I is registered behind the sample by the neutron detector.

tron beam. It is defined as the product of the microscopic cross-section σ and the atomic density N:

$$\Sigma = \sigma \cdot N \tag{2}$$

The microscopic cross-section σ represents the interaction probability of an element with the incident radiation, while the atomic density N is defined as:

$$N = \frac{\rho}{A} \cdot N_A, \tag{3}$$

where ρ is the material density, A the atomic weight and N_A is Avogadro's constant. With the attenuation coefficient Σ, it is thus possible to determine the density ρ of a specimen if the thickness is known. A detailed overview on the interactions between neutrons and wood and the attenuation coefficients of wood for cold and thermal neutrons is provided by Mannes et al. (2009).

Eq. (1) applies for objects containing only one material. For compounds containing several materials the attenuation is given by:

$$I = I_0 \, e^{-\sum_i \Sigma_i \cdot z_i}, \tag{4}$$

where i sums all materials with their respective attenuation coefficient Σ_i and layer thickness z_i. For the presented experiments, considering the tested specimens as time-dependent mixture of wood structure and water, the transmitted beam can be described as:

$$I(t) = I_0 \cdot e^{-\{\Sigma_w \cdot z_w(t) + \Sigma_h \cdot z_h(t)\}}, \tag{5}$$

where w designates the attenuation coefficient and thickness of the wood layer and h designates the attenuation coefficient and thickness of the water layer. In this context, wood and water layer have to be considered as discrete layers. The time-dependence shows in the intensity of the transmitted signal I. It reflects the changes in the layer thicknesses of the present materials, i.e., of wood and water. To separate the signal of the absorbed water from the wood signal, the images were referenced to the initial state. The time-dependence is given by:

$$z_i(t) = z_i(t_{ref}) + \Delta z_i(t). \tag{6}$$

As a reference time, the start of the experiment was chosen, where the samples were assumed to be absolutely dry, so that $z_h(t_{ref}) = 0$.

The images were referenced by dividing the time-dependent images by the initial dry state, yielding the changes between the images over time.

The wood component in Eq. (5) can be assumed to be constant, despite the swelling. While the thickness of the sample increases the atomic density of the wood (without water molecules) diminishes, the overall number of "wood atoms" along the path of the neutrons remains the same. With this and the presumption that no water is present in the reference state, the amount of water can then be calculated as the change in the water layer with:

$$\Delta z_i(t) \approx \Delta z_h(t) = -\ln\left(\frac{I(t)}{I(t_{ref})}\right) \cdot \frac{1}{\Sigma_h} \tag{7}$$

Data evaluation To evaluate the experimental data, the raw images were corrected with standard procedures common to all transmission-based methods. One such procedure is the "dark current" correction compensating the offset caused by the background noise of the CCD camera. The other is the "flat field" correction, which equalises inhomogeneities in the beam and on the scintillator screen. Furthermore, a median filter was applied on the image data to eliminate "white spots" (the result of hits by γ-particles on the CCD camera chip).

Neutrons are very susceptible to scattering, which can occur as "sample scattering" on the atoms within the specimen or as "background scattering", where neutrons are scattered by the experimental facility. The neutrons, which are scattered on the detector are registered as an additional signal and distort the recorded data. For a quantitative evaluation of the experimental data, these scattering events were corrected by the scattering correction tool QNI (Quantitative Neutron Imaging) developed by Hassanein (2006).

The corrected images were further evaluated. The images gathered in the course of the experiment were referenced on the initial dry state: they were divided by the first image of the experiment to separate the signals of wood and absorbed water along Eq. (7). The resulting referenced images represent the changes that had occurred in every pixel since the start of the experiment (Figure 4). These changes comprise not only the absorbed water but also dimensional changes. The swelling induced by the water absorption caused a dislocation of the sample edges. This made a direct quantification from the referenced images difficult and for the area of the sample edges impossible. The data had thus to be first retrieved from the images before they could be referenced. For this purpose, a line profile with almost the whole sample width was laid over the entire sample height (Figure 5). This profile yielded transmission values for every position in the vertical direction, averaged over the whole profile width. By using these averaged data, the noise was reduced and the signal smoothened. The dislocation of the edges was compensated by synchronising the transmission data rows using the slope representing the upper edge of the sample as fixed point. However, the edges show a slight blurriness as consequence to the phenomenon of geometrical unsharpness making an exact synchronisation difficult (Lehmann et al. 2007). The transmission values were subsequently converted to attenuation coefficients.

The reference curves, i.e., the profiles from the start of the experiment, where the samples were presumed to be absolutely dry, showed conspicuous peaks towards the upper end of the sample (circles in Figure 6). It was clear that the samples had already absorbed a certain amount of water during the preparation and positioning of the sample. Thus, the start of the experiment did not correspond exactly to the start of the diffu-

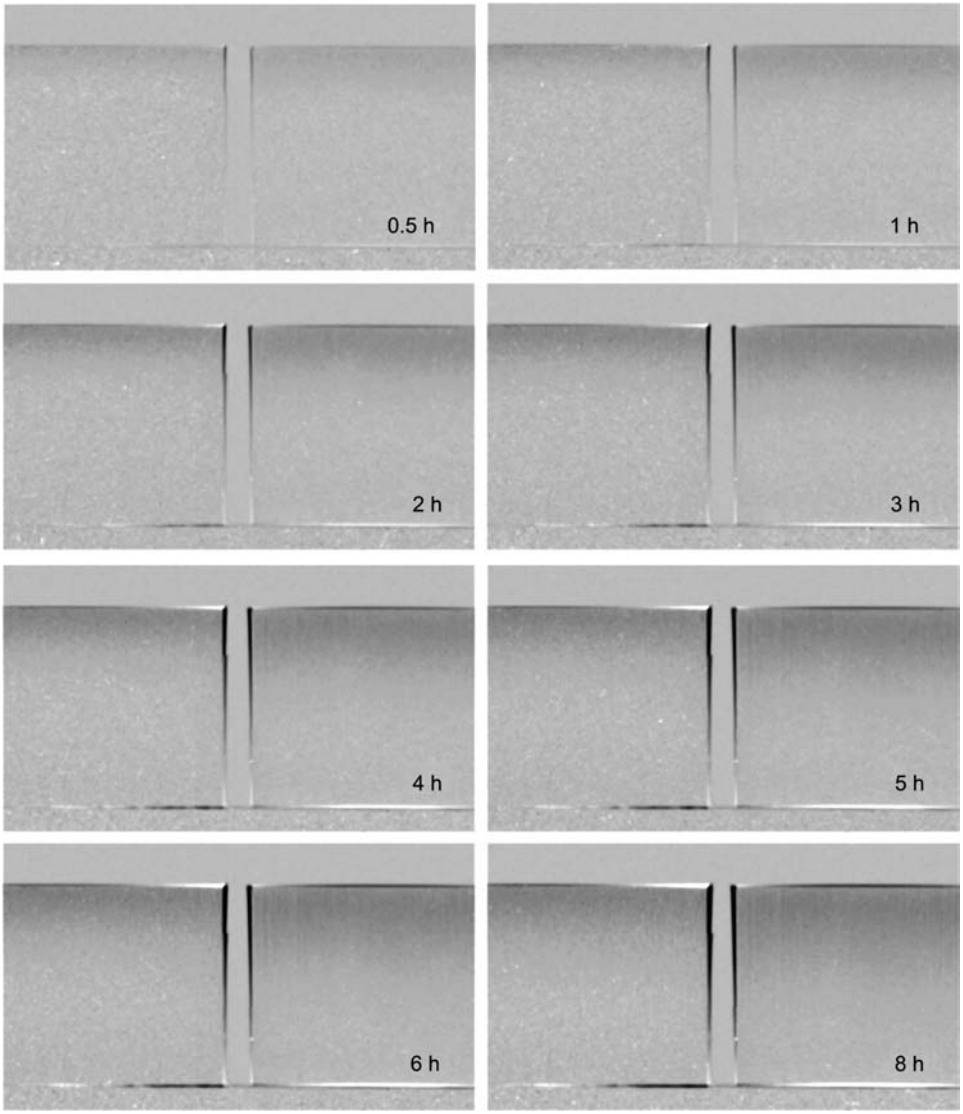

Figure 4 Dry-referenced images of samples of European beech (left) and Norway spruce (right). The water absorption from the wet climate (above the samples) is visible as broadening band of darker grey. The black and white regions at the sample edges show the dislocation of the edges due to swelling.

sion process and a temporal offset of 0.25 h for spruce and 0.1 h for beech had to be added to the time line. For the calculation of the diffusion coefficient *D*, only data from an area in the middle of the samples were taken into account (sector between vertical lines in Figure 6). This area corresponds to the penetration depths of the moisture at the start (right boundary) and the end of the experiment (left boundary); data on the left of this region (toward the dry side) were assumed to be zero and discarded because of the relatively high noise level; the right boundary corresponds to the point in the sample, which was still dry in the reference image.

In addition, an attempt was made to calculate the total water content of the sample using data over the entire range. To compensate the signal from the absorbed water on the right hand side of the dry reference state the data from the adjacent dry area was extrapolated toward the right edge, thus creating the most likely course of the attenuation coefficient values towards the end of the sample (arrows in Figure 6).

Determination of the diffusion coefficient One of the main parameters describing water transport by means of diffusion through a material is the diffusion coefficient. The diffusion itself can be defined as molecular mass flow resulting from the diffusing substance's gradient of concentration (Siau 1995).

The evaluation of the NI data yielded the water content for every pixel within the images and thus for each position within the sample. Based on these experimental results, it was possible to approximate the 1-D moisture transport by means of the second order linear partial differential equation (*PDE*) of the diffusion, which corresponds to Fick's second law:

$$\frac{\partial c}{\partial t} = \frac{\partial}{\partial x}\left(D\frac{\partial c}{\partial x}\right) \tag{8}$$

where c is the concentration, t the time, x the moisture transport direction (longitudinal) and D the concentration-dependent diffusion coefficient, given in Eq. (9) according to Olek et al. (2005):

$$D = D_0 \cdot e^{\alpha \cdot c} \tag{9}$$

where D_0 is the diffusion coefficient at initial concentration and α a constant describing moisture dependency.

As described in the previous paragraph, the experimental data were cleaned of some boundary distortions towards the upper

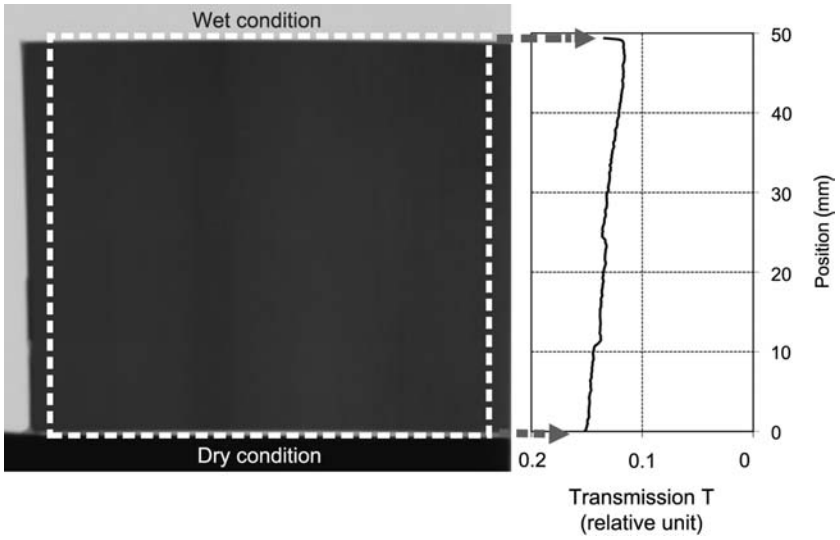

Figure 5 From the corrected neutron image, the data were retrieved with a profile almost as wide as the sample (left hand side); horizontal lines were averaged yielding a mean transmission profile over the whole height of the sample (right hand side).

edge of the samples. The initial MC in the experiment and the calculation was assumed to be zero. To calculate the diffusion coefficient, the time was adjusted by adding 0.25 h for spruce and 0.1 h for beech to the referenced data rows. Thus, Eq. (8) could be solved with the conditions in Eq. (10) for the dry and Eq. (11) for the moist boundary Γ using a MATLAB® solver algorithm for partial differential equations:

$$c(x, t) = 0 \qquad (x,t) \in \Gamma \; x \; [0,t] \tag{10}$$

$$\left(-D \frac{\partial c}{\partial x}\right) = \sigma \cdot [c(x,t) - c_{\infty}] \qquad (x,t) \in \Gamma \; x \; [b,t] \tag{11}$$

where σ is the surface emission coefficient, c_{∞} the equilibrium concentration and b represents the height of the sample. Differences between the experimental results c_{exp} and the results for the solved *PDE* c_{calc} were characterised by an objective function S:

$$S = \sum_{i=1}^{x_n} \sum_{j=1}^{t_n} (c_{\exp}(x,t) - c_{calc}(x,t))^2 \tag{12}$$

where x_n is the number of local measuring points within the calculation range (vertical lines in Figure 6) and t_n the number of time steps. Minimising S using a "Nelder-Mead simplex direct search" optimisation algorithm yielded the corresponding analysis parameters D_0, α, σ and c_{∞}.

Results and discussion

Total water content

The data from the last image (39 h) was used to verify the accuracy of the NI method. After the last image was taken, the samples were removed from the box and weighed with a digital balance. The difference between this weight and that of the start of the experiment gave the total mass of the absorbed water. A comparison with the mass calculated from the last neutron image is shown in Table 1. For both samples, the water contents determined with NI scarcely differ from the gravimetric results. The differences of approximately 3% or less are considerably smaller than the estimated measuring uncertainties that were calculated along the error propagation law. This can be due to a very conservative measuring error estimation, whereby the uncertainties are overestimated.

As the results ascertained by NI correspond very well to those determined gravimetrically, it was verified that the images made at different times during the measuring campaign contain accurate information on the actual amount and location of absorbed water within the wood sample.

The theoretically detectable minimum water content of the samples was calculated along Eq. (1) with the known attenuation coefficient of water for the thermal spectrum of NEUTRA. The calculated minimum thickness of the water layer is 30 μm. This corresponds to MC changes of 0.2% for the beech sample and 0.4% for spruce, which can be determined with NI.

The total water content within the wood samples was calculated for the first 8 h and is depicted in Figure 7. The experimentally determined mass of the absorbed water shows a clear linear correlation with $\sqrt{t}$. The linearity could be expected for the first hours of adsorption where the influence of the opposite, dry side of the specimen is negligible. The fact that the linear regression cuts the *y*-axis in Figure 7 below zero was already described by Crank (1956). This may be attributed to surface convection losses and compressive stresses on the surface (Siau 1995).

Attenuation coefficient profiles

The total attenuation coefficients include both the attenuation by wood and by water. The vertical profiles for the beech and the spruce sample are presented in Figure 6. The rapid increase over the measuring period is already conspicuous in the unreferenced data. The inhomogeneous profile with higher values in the centre of the sample, which already appear in the curve for the dry initial state, may be due to several reasons. It could be due to an inconsistent density distribution within the wood sample, which plays an important role. However, the slight

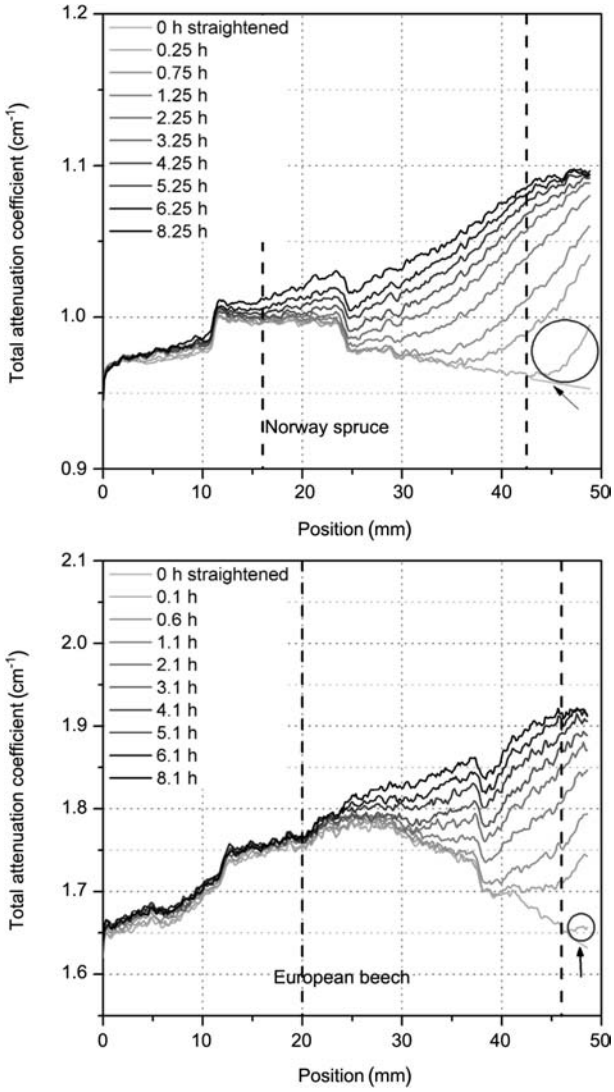

Figure 6 Vertical profiles of the attenuation coefficients over a spruce (top) and a beech sample (bottom) during the diffusion experiment; the left side represents the specimen's lower part (toward the silica gel), the right part is the upper part open to the wet climate (ca. 27°C at 86% RH); the samples had already absorbed water until the start of the experiment (circles); for the determination of the diffusion coefficient, only data between the vertical dashed lines were used; for the determination of the sample's total water content, the graphs were extended along the most likely course (arrow).

peak in the middle is at least partially caused by the isolating aluminium tape. While the aluminium itself is transparent for neutrons, the adhesive, which contains hydrogen, can attenuate the neutron beam to a certain

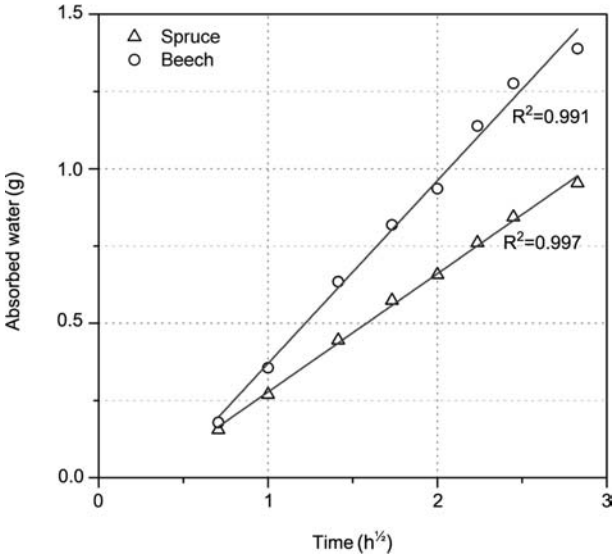

Figure 7 Mean total water content in the beech and spruce sample over time.

degree. The accumulation in the middle is due to the fact that several layers of tape had to be used as it was not as wide as the sample height.

Water concentration and diffusion coefficient

The profiles of the volumetric water concentration were calculated on the basis of the dry-referenced data (Figure 8). As mentioned in the methods section, the differences between the experimental results and the regression curves were minimised by an optimisation algorithm. For the upper part towards the wet side, the fitted curves scarcely differ from the experimental results. However, the experimental data towards the dry side lie clearly above the calculated values. This could be due to the assumption used for the calculation that the RH in this part of the samples is 0%, while the actual value was higher.

Overall, the experimental results are still in good agreement with Fick's second law. The determined diffusion coefficients and the corresponding calculation parameters for diffusion in longitudinal direction determined under unsteady state conditions for beech and spruce are presented in Table 2. Here, the results are compared to values determined by Olek et al. (2005), who used a similar analysis approach for the determination of the diffusion coefficient in beech wood. Differences between the literature values and the NI results can be accounted for by several explanations:

Table 1 Mass of absorbed water after 39 h experiment time determined by weighing and calculated from neutron imaging (NI).

	Mass determined by		Mass difference	
Wood species	Weighing (g)	NI (g)	Rel. Δ mass (%)	Rel. Δ NI (%)
European beech *Fagus sylvatica*	3.05	3.04	0.34	6.23
Norway spruce *Picea abies*	1.74	1.68	3.23	10.90

Rel. Δ mass is the difference between these data. Rel. Δ NI is the expected relative measuring uncertainty.

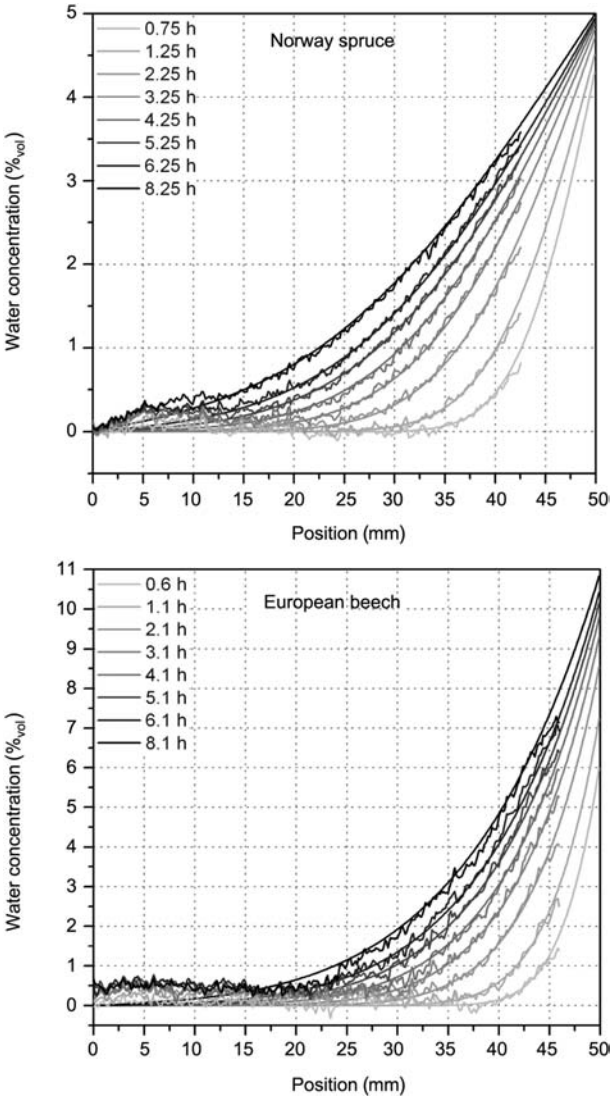

Figure 8 Vertical profiles (experimental results and the corresponding model curves) of volumetric concentration of water over the position in the spruce (top) and the beech sample (bottom) during the diffusion experiment; the left hand side represents the specimen's lower part (toward the silica gel), the right hand panel is the upper part open to the wet climate (ca. 27°C at 86% RH).

- experimental data – the NI data comprise information on location and time while the data of Olek et al. depend only on time,
- moisture boundary conditions – absolute values and influence of air flow (ventilators),
- sample thickness in diffusion direction – using only a single transport equation can yield different results for varying thicknesses (Wadsö 1994).

More publications are available for the diffusion coefficient determined under steady state conditions than under unsteady state conditions. An overview is listed in Table 3. These values are clearly lower than the ones determined with NI under unsteady state conditions. The differences can be attributed to the different experimental conditions and to the different theoretical approach chosen for the calculation. For instance, Pfriem (2007) shows a difference of factor 10 between the diffusion coefficients determined under steady and unsteady state conditions for spruce wood in tangential direction.

The approach presented in this article represents just one possibility for the evaluation of the data ascertained by NI. Other approaches could, for example, be based on a multi-Fickian model (Frandsen et al. 2007).

Conclusions

By means of NI, it was possible to quantify the water content within wood samples in a non-destructive way. In contrast to conventional methods, NI allows not only the time-dependent resolution of diffusion processes but also to localise the moisture distribution within the specimen. Based on the NI data, it was possible to ascertain the moisture-dependent diffusion coefficients for beech and spruce in the longitudinal direction. Due to the high sensitivity of NI for hydrogen, even small amounts of water (e.g., by absorption from air moisture) can be detected and quantified. The quantitative resolution for the wood MC is in the order of 0.2% for the beech sample and 0.4% for spruce.

However, the presented investigation featured some difficulties. Due to the complexity of the experiment and availability of measuring time at the NI facility, the number of samples was restricted. The experiment can only be regarded as first test series, which has to be followed by more extensive measuring campaigns with a higher number of samples. Further, during the evaluation of the data it was not possible to use the data from the sample edges. The dry-referencing was difficult in the edge areas due to geometrical unsharpness, swelling and the fact

Table 2 Determined parameters for diffusion in longitudinal direction [according to Eqs. (9) to (12)].

Wood species	ρ (g cm^{-3})	D_0 (m^2 h^{-1})	σ (m^2 h^{-1})	c_0 (%$_{vol}$)	c_∞ (%$_{vol}$)	α
European beech *Fagus sylvatica*	0.65	2.19e-5	3.27e-3	0	13.78	-5.93e-2
Norway spruce *Picea abies*	0.38	2.75e-5	17.58e-3	0	5.32	2.66e-2
European beech (Olek et al. 2005)	–	1.08e-5	1.61e-3	ca. 4.6	ca. 9.1	-1.74

ρ, oven-dry density; D_0, diffusion coefficient at initial concentration; σ, surface emission coefficient; c_0, initial concentration; c_∞, equilibrium concentration; α, constant describing moisture dependency.

Table 3 Overview over several diffusion coefficients *D* in longitudinal direction determined under steady state conditions.

Wood species	ρ (g cm^{-3})	*T* (°C)	MC (%)	*D* (m^2 h^{-1})	Reference
Wood (physical model)	0.50	28	7.5	1.26e-5	Siau 1995
Norway spruce *Picea abies*	0.40	23	4.5	9.40e-6[a]	Zillig et al. 2007
	0.40	23	9.8	8.30e-6[a]	
	0.40	23	13.3	7.10e-6[a]	
European beech *Fagus sylvatica*	0.79	35	10.7	4.30e-6	Mouchot et al. 2006
Norway spruce *Picea abies*	0.47	35	10.7	1.48e-5	

ρ, oven-dry density; *T*, temperature; MC, moisture content.
[a]Determined from the water vapour resistance factor according to Siau (1995).

that the diffusion process had already begun before the start of the experiment.

Nevertheless, NI is a method which proved to be very suitable for investigations of wood-water related processes. It allows visualising moisture transport processes in wood and can contribute to a better understanding of diffusion processes.

References

Alkan, S., Zhang, Y.L., Lam, F. (2007) Moisture distribution changes and wetwood behavior in subalpine fir wood during drying using high X-ray energy industrial CT. Drying Technol. 25:483–488.

Baettig, R., Rémond, R., Perré, P. (2006) Measuring moisture content profiles in a board during drying: a polychromatic X-ray system interfaced with a vacuum/pressure laboratory kiln. Wood Sci. Technol. 40:261–274.

Cai, Z.Y. (2008) A new method of determining moisture gradient in wood. Forest Prod. J. 58:41–45.

Crank, J. The Mathematics of Diffusion. Clarendon Press, Oxford, 1956.

Frandsen, H.L., Damkilde, L., Svenson, S. (2007) A revised multi-Fickian moisture transport model to describe non-Fickian effects in wood. Holzforschung 61:563–572.

Hassanein, R. (2006) Correction methods for the quantitative evaluation of thermal neutron tomography. Dissertation. ETH Zurich, Zurich, Switzerland.

Koc, P., Houška, M., Štok, B. (2003) Computer aided identification of the moisture transport parameters in spruce wood. Holzforschung 57:533–538.

Lehmann, E., Vontobel, P., Scherrer, P., Niemz, P. (2001a) Application of neutron radiography as method in the analysis of wood. Holz Roh Werkst. 59:463–471.

Lehmann, E.H., Vontobel, P., Wiezel, L. (2001b) Properties of the radiography facility NEUTRA at SINQ and its potential for use as European reference facility. Nondestruct. Test. Eval. 16: 191–202.

Lehmann, E.H., Frei, G., Kühne, G., Boillat, P. (2007) The micro-setup for neutron imaging: a major step forward to improve the spatial resolution. Nucl. Instrum. Meth. A 576:389–396.

Mannes, D., Josic, L., Lehmann, E., Niemz, P. (2009) Neutron attenuation coefficients for non-invasive quantification of wood properties. Holzforschung 63:472–478.

Merela, M., Oven, P., Serša, I., Mikac, U. (2009) A single point NMR method for an instantaneous determination of the moisture content of wood. Holzforschung 63:348–351.

Mouchot, N., Thiercelin, F., Perré, P., Zoulalian, A. (2006) Characterization of diffusional transfers of bound water and water vapor in beech and spruce. Maderas, Cienc. Tecnol. 8: 139–147.

Niemz, P., Lehmann, E., Vontobel, P., Haller, P., Hanschke, S. (2002) Investigations using neutron radiography for evaluations of moisture ingress into corner connections of wood. Holz Roh Werkst. 60:118–126.

Olek, W., Perré, P., Weres, J. (2005) Inverse analysis of the transient bound water diffusion in wood. Holzforschung 59:38–45.

Pfriem, A. (2007) Untersuchungen zum Materialverhalten thermisch modifizierter Hölzer für deren Verwendung im Musikinstrumentenbau. Dissertation. TU Dresden, Dresden, Germany.

Plagge, R., Funk, M., Scheffler, G., Grunewald, J. (2006) Experimentelle Bestimmung der hygrischen Sorptionsisotherme und des Feuchtetransportes unter instationären Bedingungen. Bauphysik 28:81–87.

Scheepers, G., Morén, T., Rypstra, T. (2007) Liquid water flow in *Pinus radiata* during drying. Holz Roh Werkst. 65:275–283.

Siau, J.F. (1995) Wood: influence of moisture on physical properties. Virginia Polytechnic Institute and State University, Keene NY, USA.

Skaar, C. Wood-Water Relations. Springer-Verlag, Berlin/Heidelberg/New York, 1988.

Wadsö, L. (1994) Unsteady-state water vapor adsorption in wood: an experimental study. Wood Fiber Sci. 26:36–50.

Watanabe, K., Saito, Y., Avramidis, S., Shida, S. (2008) Non-destructive measurement of moisture distribution in wood during drying using digital X-ray microscopy. Drying Technol. 26:590–595.

Wiberg, P., Morén, T.J. (1999) Moisture flux determination in wood during drying above fibre saturation point using CT-scanning and digital image processing. Holz Roh Werkst. 57: 137–144.

Zillig, W., Derome, D., Diepens, J., Carmeliet, J. (2007) Modelling hysteresis of wood. In: Häupl, P., Oloff, J. (Eds) Proceedings of the 12th Symposium for Building Physics, 29th to 31st March 2007, Institut für Bauklimatik, TU Dresden, Germany.

Received February 3, 2009. Accepted May 11, 2009.
Previously published online June 29, 2009.